IMPEDANCE/ADMITTANCE RESPONSE OF A BINARY ELECTROLYTE

J. Ross Macdonald

Department of Physics and Astronomy, University of North Carolina, Chapel Hill,
NC 27599-3255, U.S.A.

Abstract—The exact, small-signal impedance and admittance response of a fully dissociated, equi-valent material with arbitrary reaction rates and mobilities of the positive and negative charge carriers is discussed and illustrated for many different parameter values of physical significance. Although such response does not generally lead to an exact equivalent circuit using conventional circuit elements, even including finite-length Warburg diffusion elements, binary data can be fitted to the full binary small-signal response model contained in the available LEVM complex nonlinear least squares fitting program, an approach usually more appropriate than one using approximate equivalent circuits, and a procedure which leads directly to estimates of important microscopic parameters of the system. A useful approach for selecting appropriate starting values of fitting-model parameters is described and illustrated. Detailed fitting of synthetic binary response data containing random errors is illustrated by comparing the results of fits to the true binary model with fits to alternate, approximate equivalent circuit models.

Key words: impedance spectroscopy, unsupported systems, data analysis.

INTRODUCTION

Binary response occurs in materials containing a single species of positive and a single species of negative charge. Examples are unsupported liquid electrolytes [1, 2], glass electrodes, fused salts[3], solid electrolytes [4], and semiconductors. Very few graphical results for the bulk, reaction, and diffusion small-signal *ac* response of an unsupported binary electrolyte appear in the literature. For an unsupported solid material, it is often a good approximation, during the time of measurement, to take the mobility of charge of one sign as zero, but this is not always true. Especially at high temperatures, charges of both signs can often move appreciably in a half-cycle of the measuring frequency, particularly when the minimum measurement frequency is of the order of 10^{-2} Hz or less, as it often is. Of course, for unsupported binary liquid electrolytes, charges of both signs are always mobile.

Here, we are specifically concerned with the response of a binary system with charges of both signs mobile and with either or both free to react at symmetrical, plane, parallel electrodes. Although an exact small-signal expression of the impedance of such a system has been available for over a decade[5]; it is sufficiently complicated that all its implications have not yet been fully explored. In its full generality, it treats both extrinsic and intrinsic materials, arbitrary dissociation, arbitrary valence numbers, arbitrary mobilities (μ_n and μ_p), adsorption at the electrodes, arbitrary reaction rate constants (k_n and k_p), and extrinsic and intrinsic charge generation and recombination. Here the n and p subscripts denote negative and positive charges, respectively.

For simplicity, we shall here restrict attention to the fully dissociated intrinsic situation with unity valence numbers and without adsorption, one appropriate for

many solid and liquid binary electrolytes. The effect of incomplete dissociation has already been examined in some detail for the completely blocking situation [6], and, to a lesser degree, for the situation where charge of only one sign reacts at the electrodes[5, 7].

Further, nothing more needs to be said about the response of a fully dissociated intrinsic binary system with charge of only a single sign mobile and free to absorb and react at the electrodes. As Ref. [5] shows, its response is exceedingly well approximated by that of the circuit of Fig. 1 with all distributed circuit elements[8], the Z_Ds, omitted. Expressions for the circuit element in terms of microscopic quantities are presented in this reference. Note that although bulk effects (the high frequency limiting resistance, R_∞, and the geometrical capacitance, C_g), electrode reaction effects (the reaction resistance, R_R, and the
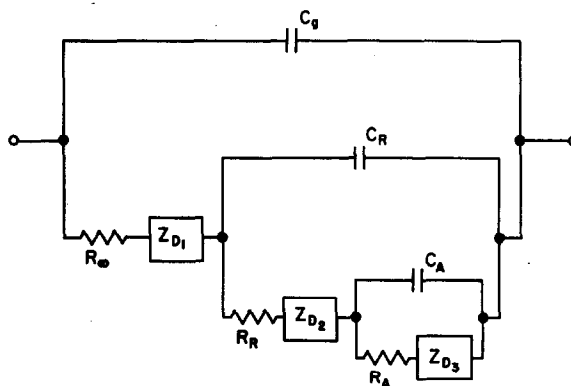

Fig. 1. Equivalent circuit often appropriate for fitting impedance spectroscopy data when bulk, reaction (C_R, R_R), adsorption (C_A, R_A), and possibly one or more distributed processes are present.

reaction, or double-layer, capacitance, C_R), and adsorption effects (the adsorption resistance, R_A, and the adsorption capacitance, C_A) may all be present, there are no diffusion effects for uni-mobile materials.

For the present situation, an equivalent circuit is unnecessary since the impedance expression obtained from the exact small-signal response equations may be used directly for plotting or data-fitting purposes. In general, the impedance frequency response thus obtained is sufficiently complicated that it cannot be well approximated by that of an equivalent circuit, even one involving several finite-length Warburg diffusion elements. The exact impedance expression is thus likely to be superior to equivalent circuits used to fit appropriate binary-electrolyte data, such as that of Ref. [3] for a molten salt. An aim of the present work is to illustrate some aspects of the exact response and describe how it may be directly employed for data fitting to yield more microscopic parameters of the system than possible with usual equivalent circuits.

In the next section, pertinent parameters of the response are described, and actual graphical complex-plane responses generated with the simulation facility of the LEVM fitting program are illustrated and discussed in the following section. Finally, fitting of binary data is considered in detail.

PERTINENT PARAMETERS AND SIMPLE RESPONSE

The following parameters are needed to characterize the present results: first, the ratio of mobilities, $\pi_m \equiv \mu_n/\mu_p$, and second, the normalized reaction rates, $\rho_n \equiv (L/2)(k_n/D_n)$ and $\rho_p \equiv (L/2)(k_p/D_p)$. Here, L is the effective electrode separation, and the Einstein relation between a diffusion coefficient, D, and the corresponding mobility, μ, is $D = (kT/e)(\mu/z) = (RT/F)(\mu/z)$, where k is Boltzmann's constant, e is the proton charge, R is the gas constant, F is the Faraday constant, T is the absolute temperature, and z is the valence number of the mobile charge. In addition, we define $M \equiv L/2L_D$, the number of Debye lengths, L_D, in the half-cell. Here we wish to deal with cells with macroscopic electrode spacing rather than with very thin membranes, so we shall take $M = 10^4$ for all our calculations. The exact results[5] apply, however, for any M value. Our graphical results would be essentially the same for a larger M.

We shall present results at the impedance or admittance level, normalized by R_∞ or $G_\infty \equiv R_\infty^{-1}$, respectively. All results apply for unit electrode area. Thus, if Z_T is the total impedance of the system, $Z_{TN} \equiv Z_T/R_\infty$ and $Y_{TN} \equiv Z_{TN}^{-1}$. Here $R_\infty = [(ec_o/L)(\mu_n + \mu_p)]^{-1}$, where c_o is the common bulk value of the concentration of positive, p_o, and negative, n_o, charge carriers. It will also sometimes be useful for plotting purposes to normalize with the normalized dc resistance of the system, $R_{DN} \equiv [\text{Re}(Z_{TN})_{\omega=0}]/R_\infty$, where ω is the angular frequency of the sinusoidal excitation applied to the system. R_{DN} is given by[5]

$$R_{DN} = \left[\frac{1}{(1 + \pi_m)(1 + \rho_p^{-1})} + \frac{1}{(1 + \pi_m^{-1})(1 + \rho_n^{-1})} \right]^{-1}. \quad (1)$$

For such normalization we shall use a lower-case subscript n. Thus, $Z_{Tn} \equiv Z_{TN}/R_{DN} \equiv Z_T/R_D$, and its real part is unity at $\omega = 0$. Because of the complexity of the full expression for Z_{TN} for even the present simplified situation, we shall not present it here and will instead give only the much simpler result for $\pi_m = 1$. Note, however, that the exact expression is also considerably simplified for completely blocking conditions and its response has been considered in detail recently[6]. The full expression for arbitrary electrode-reaction conditions, including adsorption and degree of dissociation, has been incorporated into the LEVM complex nonlinear least squares (CNLS) program available from the author's department at nominal cost. Thus, it can now be used directly for fitting small-signal binary response data [1, 3, 6, 9, 10].

The geometrical capacitance C_g is given by $\epsilon/4\pi L$, where ϵ is the dielectric constant of the material between the electrodes. Let $\Omega \equiv \omega R_\infty C_g$, the normalized frequency; for most impedance spectroscopy experiments, $\Omega_{max} < 1$. Following Ref. [5] let us define $\rho_a \equiv (\rho_n + \rho_p)/2$, $\theta_2 \equiv \sqrt{i\Omega}/2[\pi_m^{1/2} + \pi_m^{-1/2}]$, $\gamma_2 \equiv (M\theta_2)\text{ctnh}(M\theta_2)$, and $t_1 \equiv [(1 + \theta_2^2)^{1/2} M]\text{ctnh}[(1 + \theta_2^2)^{1/2} M]$.

Now we write the general Z_{TN} in terms of a part arising from R_∞ and C_g, and a part representing the rest of the response (eg everything beyond R_∞ in Fig. 1), $Z_s \equiv Y_s^{-1}$. In normalized form the general result is[5]

$$Z_{TN} = (1 + Y_{SN})/[Y_{SN} + i\Omega(1 + Y_{SN})]. \quad (2)$$

Finally, in the special $\pi_m = 1$ case, from equation (35) of Ref. [5] we can express Y_{SN} as

$$Y_{SN} = \frac{\rho_a \gamma_2 + \rho_n \rho_p}{\rho_a + \gamma_2} + \frac{i\Omega t_1}{1 + i\Omega}. \quad (3)$$

For $\Omega \ll 1$, the second term in equation (3), multiplied by G_∞ to remove its normalization, is just $i\omega C_g[(M)\text{ctnh}(M) - 1] \equiv i\omega(0.5C_{DL} - C_g]$, where C_{DL} is the conventional double layer capacitance, $\epsilon/4\pi L_D$ for large M. Since there is a C_{DL} localized near each of the identical electrodes, $C_R = 0.5C_{DL}$ is the result of two such capacitances in series[9]. Our present results are easily modified to apply to a half-cell rather than a full one. Although we shall here be concerned mostly with situations where the mobility ratio is quite different from unity, the present exact results for the $\pi_M = 1$ situation show that even here an equivalent circuit formed from conventional elements is inappropriate, and, in addition they may be used for fitting when, in fact $\pi_m = 1$.

For arbitrary π_m, we define

$$A^{1/2} \equiv (M/2)[\pi_M^{1/2} + \pi_M^{-1/2}](\Omega)^{1/2}. \quad (4)$$

Then γ_2 may be written as[5, 9, 10]

$$\gamma_2 = [iA]^{1/2}\text{ctnh}[iA]^{1/2}, \quad (5)$$

an expression of just the form of finite-length diffusion for a single reacting species in the supported situation. Thus the γ_2 terms in equation (3) can produce diffusion effects in the overall Z_{TN}. Only when ρ_n or ρ_p is infinite, however, does γ_2 appear by itself in equation (3). Then, at the impedance level, for the present $\pi_m = 1$ situation, $Z_D \equiv 1/(G_\infty \gamma_2)$ is given by

$$Z_D = R_\infty \tanh[iA]^{1/2}/[iA]^{1/2}, \quad (6)$$

again, the usual form for finite-length diffusion [5, 9–11]. In the $\pi_m \neq 1$ case, a good approximation for Z_{DN} when $(\rho_p, \rho_n) = (0, \infty)$ has been found to be[5]

$$Z_{DN} = \pi_m^{-1} \tanh[iA]^{1/2}/[iA]^{1/2}, \qquad (7)$$

which is consistent with equation (6) when $\pi_m = 1$. The acronym FLW, finite-length Warburg, will be used for the responses of equations (6) and (7). The A term appropriate for the binary electrolyte has been compared elsewhere[10, 11] with that for a supported case with a charge of only one sign reacting and detailed agreement found. Note that results for (ρ_p, ρ_n) and given π_m are also found, as one would expect from symmetry, for the (ρ_n, ρ_p) situation with $\pi_m \rightarrow \pi_m^{-1}$.

GRAPHICAL RESULTS

Although it is impractical to illustrate all the possibilities and curve shapes produced when π_m, ρ_n, and ρ_p are all free to vary, Figs 2–6 shows many representative responses plotted in the normalized impedance or admittance plane. Figures 2–4 all have π_m fixed at 10^{-4} so the mobility of negative charges is far less than positive ones. The arrows indicate the direction of increasing frequency. In Fig. 2, ρ_n is fixed at ∞ and ρ_p varies. Note that R_{DN} normalization is used here in order to show comparative curves shapes and that the normalizing values are given in the figure caption. In these graphs, quantities like $(10^{-4}, 3)$ indicate values of (ρ_p, ρ_n).

The $(0, \infty)$ curve of Fig. 2, where the high-mobility charges are completely blocked and the low-mobility ones react very rapidly, is essentially that of standard finite-length diffusion response. It is very closely approximated by the Z_{DN} expression of equation (7). It follows that $R_{DN} = 1 + \pi_M^{-1} = 10,001$ for this situation. The 1 here, corresponding to R_∞ when R_{DN} is unnormalized, is the width on the real impedance axis of the semi-circle arising from the bulk response, that of R_∞ and C_g. It is far too small to appear separately in Fig. 2 except for the $(10^{-1}, \infty)$ response curve. As Fig. 2 and the normalizing values indicate, when ρ_p increases from zero the diffusion curve rapidly decreases in absolute size and in relative maximum

Fig. 3. The normalized total impedance, $Z_N \equiv Z/R_\infty$, plotted in the impedance plane for $\pi_m = 10^{-4}$ and a variety of (ρ_p, ρ_n) choices.

height until by $\rho_n \gtrsim 10^{-3}$ there is a long, nearly flat, response region, quite different from ordinary finite-length diffusion response.

In Fig. 3, which uses R_∞ normalization, the true relative sizes of the curves appear for four different (ρ_p, ρ_n) choices. Note that the ρ_p of the $(10^{-4}, 0)$ curve has been selected to produce very nearly the same R_{DN} value as that for $(0, \infty)$, but the first curve is just a full reaction semicircle without diffusion effects and the second is a diffusion curve without reaction effects. By contrast, the $(10^{-4}, 3)$ curve involves contributions from both processes. The input choices for Fig. 4 are similar to those for Fig. 3, but in Fig. 4, ρ_p is fixed at 10^{-4} for all the curves, and we see the transition from all-reaction response to all–diffusion response as ρ_n increases from 0 to ∞.

In Fig. 5 we have set $\rho_n = \infty$ and $\pi_m = 10^{-2}$. Since R_∞ normalization is used here, the variation in ρ_p changes the size, and, of course, the shape of the impedance curves appreciably. But note that the sizes and shapes of the corresponding admittance curves change much less. Thus, it is clear that for situations like this impedance plane plots will yield more information than will admittance plane ones.

Detailed analysis and circuit fitting has already been published for the binary electrolyte with $(0, \rho_n)$ for $0 < \rho_n \leqslant \infty$ and a wide range of π_m values[7], so this situation needs little further discussion here. It is, however, worth pointing out that it was found that response calculated from the exact small-signal solution could not be well fitted by the Fig. 1 circuit with no Z_Ds and with conventional expressions for the reaction circuit components. Expressions for these
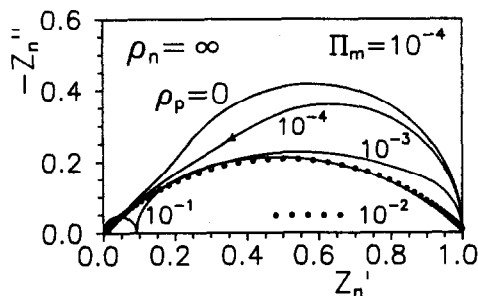
Fig. 2. The normalized total impedance, $Z_n \equiv Z/R_{DC}$, plotted in the impedance plane for $\pi_m = 10^{-4}$, $\rho_n = \infty$ and a variety of ρ_p values. The $\rho_p = 10^{-2}$ curve is defined by the open circles in order to distinguish it from the solid $\rho_p = 10^{-1}$ curve. The five normalizing values of R_{DN}, beginning at $\rho_p = 0$, are 10,001, 5000.75, 910.008, 100.0001, and 10.989.
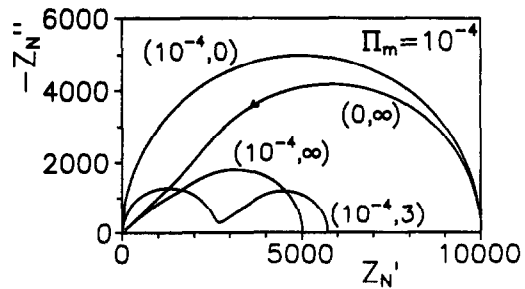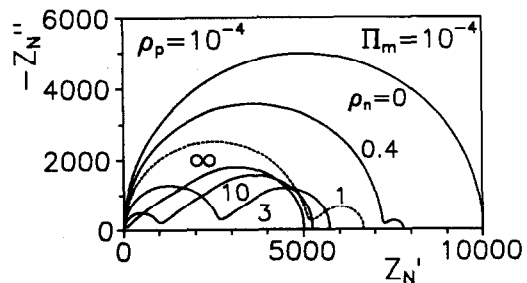
Fig. 4. The normalized total impedance Z_N plotted in the impedance plane for $\pi_m = 10^{-4}$, $\rho_p = 10^{-4}$, and a variety of ρ_n values.
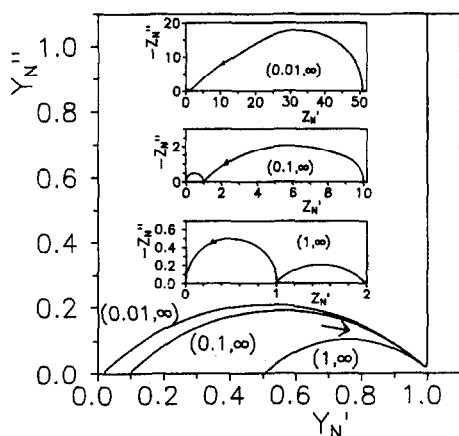
Fig. 5. Separate impedance plane plots for three choices of ρ_p and the corresponding curves in the admittance plane. Here $\pi_m = 10^{-2}$ and $\rho_n = \infty$.

quantities involving M, π_m, and ρ_n were found, however, that allowed good fits and thus good estimates of such parameters as reaction rates. For the $(0, \infty)$ case, the standard finite-length-diffusion curve shape of equation (7) applied well for a wide range of π_m. Admittance curve plots presented in the earlier work[7] showed, however, that the curve shapes in this plane depended strongly on π_m. For such fitting, the circuit of Fig. 1 was used with $Z_{D1} = Z_{D2} = 0$ and Z_{D3} given by the Z_D of equation (7).

Finally, Fig. 6 presents impedance and admittance plane plots for several values of π_m and the choice $(0.1, \infty)$. Note the R_{DN} normalization for the impedance curves. Here we see that for $\pi_m < 1$ the shape of the low frequency arc is far from the normal finite-length-diffusion arc apparent for $\pi_m = 1$. As in Fig. 2, a reaction semi-circle and a finite-length-diffusion arc meld together to yield curve shapes unlike those of either separately. The admittance-plane plots show appreciable dependence on π_m and,
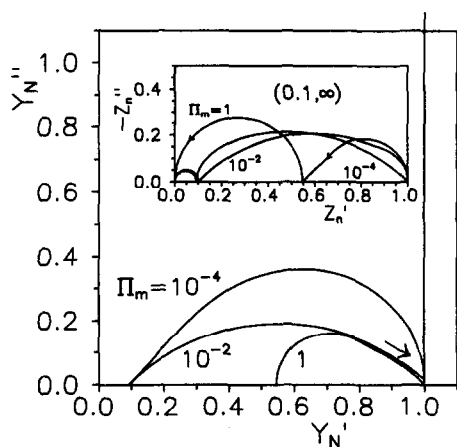

Fig. 6. Impedance and admittance plane plots for $(0.1, \infty)$ and several π_m values. Note the use here of R_{DN} normalization for the impedance plots and R_∞ normalization for the admittance ones. The three normalizing values of R_{DN} for $\pi_m = 10^{-4}$, 10^{-2}, and 1 are, respectively, 10.989, 10.009, and 1.982.

for $\pi_m = 1$, the admittance curve looks much like a reversed impedance-plane finite-length-diffusion curve. Note that in all the admittance plots presented herein, the high-frequency spike appearing at $Y'_N = 1$ has been chopped off at the top of the figure. It arises from C_g and causes Y''_N to approach ∞ as $\omega \to \infty$.

Although only a limited set of binary electrolyte responses has been included herein, they give some idea of the richness of complex-plane curve shapes possible for such a system. With the present availability of the exact binary response[5] incorporated in the LEVM CNLS fitting program[10, 12] one need no longer attempt to fit to an approximate equivalent circuit but can now fit binary response data directly to this model and thus obtain estimates of important material parameters such as k_n, k_p, μ_n, μ_p, c_o, and ϵ, as demonstrated in the next section. Only if one or more of the material parameters of the system are appreciably distributed is such fitting likely to fail, then fitting to an equivalent circuit will still be necessary.

DATA FITTING

(a) Fitting the proper model

When it is known or suspected that data to be analysed involve a binary situation, the binary-model fitting choices available in the LEVM program may be used for either a completely blocking situation or a partly conducting one. But since an equivalent circuit is usually inappropriate for such data, how should their analysis proceed? Although a discussion of the transformation of binary fitting parameters to microscopic quantities is presented in Section V of Ref. [5], obtaining adequate initial parameter estimates for such further analysis may not always be straightforward. Therefore, an actual ab initio data fitting is illustrated here in order to demonstrate some of the fitting procedures available and appropriate for binary data.

We shall purposely illustrate the fitting of data which are more ambiguous and less accurate than average in order to demonstrate a difficult fitting situation. Although exact binary data and data with random errors will be generated for fitting, so that all parameter values are known, we begin the data fitting without any prior parameter knowledge, just as one might for real data. We assume, however, that valence numbers are unity and that we are dealing with a fully dissociated situation, but LEVM can handle more complicated situations as well.

We shall consider data which yield a complex plane plot like that in the top block of Fig. 5. The arc shape suggests that the dominant process in finite-length diffusion, perhaps occurring not in a binary system but in a supported electrolyte. Then the Z_S response would be of the general form of equation (6) with R_∞ replaced by R_W and A by $\omega\tau_W$, where R_W and τ_W are unknown diffusion parameters. For generalized finite-length Warburg response[8] (GFLW), the 0.5 exponents in equation (6) would be replaced by the free parameter ψ_W, where $0 \leqslant \psi_W < 1$. Further, the data shape is also of the form expected from Davidson–Cole (DC) response at the Z level. Its appropriate Z_S expression is[13]

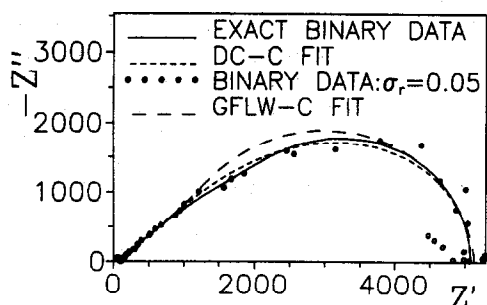$$Z_S = R_{DC}/(1 + i\omega\tau_{DC})^{\beta_{DC}}, \qquad (8)$$

Fig. 7. Impedance plane plot of exact binary data, Davidson–Cole fit to the exact data, binary data with proportional errors (points only), and generalized finite-length Warburg fit to the exact data. See Table 2.
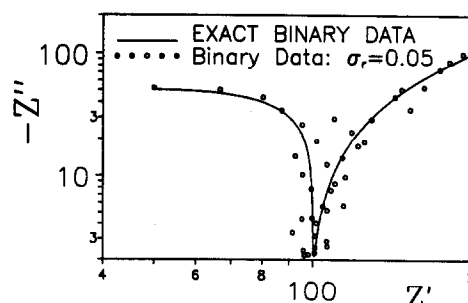

Fig. 8. Log–log impedance plane plot in the high-frequency region of the exact binary data and of the data with $\sigma_r = 0.05$ proportional errors.

with $0 \leqslant \beta_{DC} \leqslant 1$. These fitting possibilities will be investigated below in addition to binary-model fitting.

We shall fit to exact data, to data containing small proportional random errors ($\sigma_r = 0.01$) and to data incorporating appreciably larger proportional random errors ($\sigma_r = 0.05$), larger than commonly encountered in practice. If $Z_e'(\omega_i)$ is an exact value of the real part of the impedance, then the corresponding value with proportional error is $Z'(\omega_i = Z_e'(\omega_i)[1 + \delta_i]$, where δ_i is an independent random sample from a normal distribution with zero mean and a standard deviation of σ_r. The errors in the imaginary values of Z are formed in the same way but with an entirely independent set of δ_is having zero mean and the same σ_r.

The unnormalized impedance plane plot for the exact data we shall use is shown in Fig. 7 and covers an angular frequency range of $10^{-5}–10^6 \, s^{-1}$. The separate points present in the figure are for the data with $\sigma_r = 0.05$. Such data will be referred to as containing 5% proportional errors, but since the actual errors are drawn from a normal distribution a few of them may be as large in magnitude as 10 to 20%. Now, in order to carry out a binary-model-fit of the 5% data (the hardest of the three sets of data to fit), one needs initial guesses for the following parameters: R_∞, C_g, M, π_m, ρ_p, and ρ_n. Since all quantities are given per unit area here, impedance and resistance units are ohm cm^2 and capacitance units are farads cm^{-2}. For simplicity, they will be suppressed hereafter.

Examination of the Fig. 8 plot and the data in the high-frequency range where the cusp occurs suggests that the initial values $R_\infty = 104$ and $C_g = 1.2 \times 10^{-8}$ would be reasonable. Only approximate values are needed. Because of the high resolving power of LEVM fitting, initial values of most of the parameters can be incorrect by 10 times or more and convergence will still be obtained, although the more parameters to be determined and the worse the data, the closer the parameter initial values need to be to their final ones for immediate convergence to occur. To demonstrate LEVMs resolving power or lack of it, we shall actually choose somewhat worse starting parameter guesses than the data suggest.

Next, since we assume or know that the data are associated with a cell of macroscopic rather than microscopic size, we expect that the electrode separation distance will contain many Debye lengths. Therefore, use a minimum choice of 100 for M. Comparison of the complex plane shape with that of the top block in Fig. 5 suggests that ρ_p should be small and ρ_n very large. Thus, initial choices of 0.1 and 10^9 (or any value greater than 10^5) seem reasonable. We shall hold ρ_n fixed and only later test the validity of its choice. Finally, the above comparison suggests that π_m should be less than unity. If we initially ignore π_m compared to unity, we can use equation (1) for R_{DN} to obtain an improved starting estimate for ρ_p. From the data and the above estimate for R_∞, $R_{DN} \sim 50$. Then equation (1) leads to the approximate estimate $\rho_p = 0.02$, which we shall use. Finally, we pick $\pi_m = 0.1$, larger than one might guess from the comparison or from consistency with equation (1) but chosen to make the fit more difficult.

The first line in Table 1 shows the above choices. Since the $\sigma_r > 0$ data contain proportional random errors, it is appropriate and desirable to use function-

Table 1. Steps in the complex nonlinear least-squares fitting of binary data with $\sigma_r = 0.05$ to the binary response model

Run no.	R_∞	C_g	M	π_m	ρ_p	Number of iterations
1 in	104	1.2×10^{-8}	100	0.1	0.02	n.c.
2 in	(104)	(1.2×10^{-8})	100	0.1	(0.02)	20
2 out	104	1.2×10^{-8}	1.16×10^4	5.87×10^{-3}	0.02	—
3 in	(104)	(1.2×10^{-8})	1.16×10^4	5.87×10^{-3}	0.02	7
3 out	104	1.2×10^{-8}	9.22×10^3	1.06×10^{-2}	1.05×10^{-2}	—
4 in	104	1.2×10^{-8}	9.22×10^3	1.06×10^{-2}	1.05×10^{-2}	6
4 out	100.8	1.017×10^{-8}	9.96×10^3	1.017×10^{-2}	1.012×10^{-2}	—

Parameter values shown within parentheses were held fixed during fitting. Here n.c. indicates no convergence, and the number of iterations equals the number of function evaluations required for convergence.

Table 2. Fit results for fitting of binary data with different values of σ_r to (a) the proper binary (B) model, (b) an approximate equivalent circuit involving a finite-length Warburg element (FLW or GFLW) and a parallel capacitor, C_R and (c) an approximate equivalent circuit involving a Davidson–Cole distributed element and a parallel capacitance, C_R

Fit model	σ_r	S_F	FQF	R_∞	C_g	B: M / FLW: R_W / DC: R_{DC}	τ_m / τ_w / τ_{DC}	ρ_p / ψ_w / β_{DC}	C_R
B	0	1.5×10^{-13}	-8425	$100\|2 \times 10^{-14}$	$10^{-8}\|6 \times 10^{-14}$	$10^4\|4 \times 10^{-14}$	$0.01\|8 \times 10^{-14}$	$0.01\|1.0 \times 10^{-13}$	—
B	0.01	0.0098	-650	$99.6\|1.5 \times 10^{-3}$	$10^{-8}\|4.0 \times 10^{-3}$	$9.95 \times 10^3\|2.6 \times 10^{-3}$	$0.0099\|5.0 \times 10^{-3}$	$0.0099\|6.8 \times 10^{-3}$	—
B	0.05	0.0494	-146	$100.8\|7.5 \times 10^{-3}$	$10^{-8}\|0.020$	$9.96 \times 10^3\|0.013$	$0.010\|0.025$	$0.0101\|0.034$	—
FLW	0	0.0983	54	$99.8\|0.018$	$9.32 \times 10^{-9}\|0.052$	$5732\|0.011$	$1.02 \times 10^3\|0.018$	(0.5)	
GFLW	0	0.0646	-68	$98.7\|0.012$	$9.06 \times 10^{-9}\|0.035$	$5170\|9.8 \times 10^{-3}$	$1.08 \times 10^3\|0.014$	$0.477\|3.5 \times 10^{-3}$	
GFLW-C	0	0.0516	-131	$99.8\|8.0 \times 10^{-3}$	$1.004 \times 10^{-9}\|0.020$	$5103\|7.9 \times 10^{-3}$	$1.079 \times 10^3\|0.011$	$0.471\|3.2 \times 10^{-3}$	$5.5 \times 10^{-5}\|0.081$
DC-C	0	0.0217	-401	$99.9\|3.4 \times 10^{-3}$	$9.98 \times 10^{-9}\|9 \times 10^{-3}$	$4994\|3 \times 10^{-3}$	$884\|6.4 \times 10^{-3}$	$0.480\|1.7 \times 10^{-3}$	$4.68 \times 10^{-5}\|0.045$
DC-C	0.01	0.0233	-380	$99.5\|3.6 \times 10^{-3}$	$1.004 \times 10^{-8}\|9.7 \times 10^{-3}$	$5008\|3.2 \times 10^{-3}$	$883\|6.8 \times 10^{-3}$	$0.481\|1.8 \times 10^{-3}$	$4.58 \times 10^{-5}\|0.049$
DC-C	0.05	0.0523	-127	$100.7\|8.1 \times 10^{-3}$	$1.013 \times 10^{-8}\|0.021$	$4962\|7.2 \times 10^{-3}$	$884\|0.015$	$0.481\|4 \times 10^{-3}$	$4.62 \times 10^{-5}\|0.12$

Here S_F and FQF are measures of goodness of fit. Quantities written in the form A|B denote a parameter estimate (A) and its estimated relative standard duration (B).

proportional weighting (FPWT) for the fitting, a choice that matches the input errors as well as possible and leads to parameter estimates with appreciably smaller bias than the other weighting possibilities[10]. When a binary-model fit was attempted with all five parameters free (run 1), no convergence was found. Now let numbers in parentheses indicate fixed parameter values. Run 2 indicates that convergence was achieved with 20 function evaluations. The result of the fit is listed in line 3. Next ρ_p was set free and run 3 carried out. Its results were used in run 4 with all five parameters free, leading to the last line in the table.

When all five parameters are fixed and only ρ_n is taken free, one obtains a fit estimate of it of $1.1 \times 10^6|17$. The first number is the estimate and the second is its relative standard deviation (RSD), termed the coefficient of variation by statisticians. When this value of ρ_n is taken free, along with the five of the table, their new estimates are essentially unchanged and one obtains for ρ_n the result $8.6 \times 10^5|16$. The very large value of the RSD in these fits indicates that the actual estimates of ρ_n above are completely untrustworthy. On the other hand, their large values still indicate that a large fixed value of ρ_n is indeed appropriate. This conclusion is confirmed by the results of runs like that of run 4 of the table with ρ_n fixed at various values. With $\rho_n = 100$, the ρ_p estimate is less than 10^{-8} and completely uncertain. Results approaching those of run 4 are obtained for $\rho_n > 10^4$ and are quite close to the run 4 estimates for $\rho_n = 10^5$. Thus, the value of ρ_n of 10^9 used hereafter is indeed appropriate. This value was, in fact, used in generating the exact binary data.

Now, how good is the run 4 fit and how appropriate are its estimates? This question is answered by the first three lines in Table 2, where B stands for the binary fitting model. Line 1, a fit to the exact data, yields the parameter values used to generate the data, all of which show neglible RSDs. In this table S_F is the standard deviation of the fit itself, a measure of the goodness of fit. For proportional weighting, it should be an excellent estimate of σ_r[10]. Another more sensitive estimate of goodness of fit listed in the table is the fit quality factor (FQF)[14, 15]. The smaller (algebraically) the value of FQF, the better the fit. Comparison of the fit results of lines 2 and 3 shows that although the RSDs of the parameter estimates increase by a factor of five, as they should, when σ_r increases from 0.01 to 0.05, the estimates themselves remain remarkably close to their no-error values, even for the quite irregular $\sigma_r = 0.05$ data. The parameter estimates of the third line in Table 2 are, of course, identical to those of the last line of Table 1. Finally, note that the S_F values are indeed very close to the σ_r values.

There is a built-in procedure in LEVM that transforms binary fitting parameter values to corresponding microscopic ones. When it is used with the values in line 1 of Table 2, along with a value of the absolute temperature (here taken to be 300K), it yields the following results: $\epsilon/L = 112.9$ cm^{-1}; $n_o L = p_o L = c_o L = 3.23 \times 10^{14}$ cm^{-2}, $\mu_n/L^2 = 1.915$ s^{-1} V^{-1}, and $\mu_p/L^2 = 191.5$ s^{-1} V^{-1}. The corresponding results for the $\sigma = 0.05$ fit are still very close: 114.8, 3.26×10^{14}, 1.916, and 188.3, respectively. In an

actual experimental situation, a good independent estimate of L will be available, so values of ϵ, c_0, μ_n and μ_p can be calculated. Since $\rho_p = (L/2)(k_p/D_p)$, one can use the Einstein relation to obtain D_p from μ_p and then calculate the reaction rate constant k_p using the value of ρ_p found from the fitting. Note that even when values are known for all these parameters, one cannot calculate all the parameters of an equivalent circuit such as that of Fig. 1 from them. In the present case, one can, however, calculate[5, 9] corresponding values of R_R and C_R, but their use, along with the values of R_∞ and C_g, and a FLW distributed response element for the Z_{D2} of Fig. 1, does not lead to a circuit which can closely represent the binary data, as demonstrated below.

(b) Alternative model fitting

Although the foregoing results demonstrate unequivocally that LEVM can be used to obtain excellent binary-model fitting results for a difficult data situation, what about the usual bane of impedance spectroscopy CNLS fitting: model ambiguity? We have purposely chosen a data set where such ambiguity seems likely. How well can it be resolved? Although the binary model is the correct one for these data, can other models yield as good fits, especially for data with errors? This question is answered by the results of the remaining lines of Table 2; the lines marked FLW and GFLW contain fitting results to the exact binary date for finite-length-Warburg-diffusion model response and for generalized finite-length Warburg response. We see that even without data errors these models yield quite inadequate fits. What value should we expect for R_W and τ_W? Using the exact data, the first quantity should equal $R_D - R_\infty$, here equal to about 4975. If equation (4) were applicable to this situation, it would predict a value of τ_W of about 2550 instead of the values near 1000 actually shown in the table.

Now, it is found that an appreciably better fit is obtained if the diffuse double layer capacitance, C_R in Fig. 1, is taken non-zero. Then, the full equivalent circuit involves R_∞, C_g, and a Z_S made up of the parallel combination of C_R and the GFLW expression. Results for fitting this model, designated GFLW-C, are shown in the table. The fit is much better, and although the RSD of C_R is appreciable, the C_R estimate is still statistically significant. The presence of C_R improves the low-frequency part of the fit considerably, but, as shown in Fig. 7, there is still an extensive middle-frequency region where the fit is poor. How well does the value of C_R accord with our expectations? For a large M value, $C_R/C_g = M/2$, as already discussed, a result[5] independent of the value of π_m when it is neither 0 nor ∞. In the present situation the theoretical C_R is thus 5×10^{-5}, close to the fit value. Incidentally, when the reaction resistance R_R was included as a free parameter in the fitting, along with the other six free parameters, LEVM drove its estimate down toward zero with a vary large estimated RSD. Thus, its presence is inappropriate.

We now turn to fitting results obtained using the Davidson–Cole distributed response element. Since again it was found that the presence of C_R improved the fit, it was taken as a free parameter as above, and all the DC results in the table are designated as

DC-C. The DC-C line in the table for $\sigma_r = 0$ is a much improved fit compared to the GFLW-C one for the same exact data. Its response is shown in Fig. 7, and, although it is quite close to the exact-data line, its deviation from this line is an illustration of systematic error entirely arising from the choice of a wrong fitting model. The last two DC-C lines in the table show what happens when both systematic and random errors are present. On comparing these results to the corresponding binary-fit lines in the table, we see that for $\sigma_r = 0.01$ it is still quite clear that the binary fit is much more appropriate than the DC-C one. At $\sigma_r = 0.05$, however, the differences in goodness of fit are much less substantial and, although one would still pick the binary fit as best, especially since it requires only five free parameters instead of the six of the DC-C, the choice is no longer overwhelming. Clearly for sufficiently larger random errors, one will no longer be able to make a meaningful choice.

The above results suggest that when fitting either binary or non-binary impedance spectroscopy data one should carry out as accurate measurements as possible. One should use the data, its impedance plane plots (and possibly plots at the complex modulus and/or admittance levels as well), and fitting model information to determine best estimates of the starting parameters of the model. If fitting convergence does not occur with these estimates all taken free, some or most of them should be held fixed while a few free parameter values are estimated from convergent fits. Then, more and more of the parameters should be taken free until convergence is obtained with all of them free.

It is very important, in order to obtain low-bias parameter estimates, that CNLS fits be carried out with the proper weighting. Luckily, LEVM has a facility that allows one to determine, during the least-squares fitting itself, estimates of the most appropriate values of the parameters of the weighting model as well as the fitting model[10]. When it is invoked, one need not determine weights subjectively. In the present work, this approach was not required since it was known that any errors in the data were of proportional random character. As a test, however, when a weighting model parameter which determines the fractional power of the model values used in calculating the weights was taken free, its LEVM estimate confirmed that proportional weighting was indeed the most appropriate choice for the present data with errors.

REFERENCES

1. J. H. Sluyters, *Rec. Trav. Chim.* **82** 100 (1963).
2. J. R. Macdonald, *J. electroanal. Chem.* **32**, 317 (1971).
3. C.-T. Liu and O. F. Devereux, *J. electrochem. Soc.* **138**, 386 (1991).
4. J. R. Macdonald and G. B. Cook, *J. electroanal. Chem.* **193**, 57 (1985).
5. J. R. Macdonald and D. R. Franceschetti, *J. chem. Phys.* **68**, 1614 (1978).
6. J. R. Macdonald, *J. electrochem. Soc.* **135**, 2274 (1988).
7. J. R. Macdonald and C. A. Hull, *J. electroanal Chem.* **165**, 9 (1984).
8. R. L. Hurt and J. R. Macdonald, *Solid St. Ionics* **20**, 111 (1986).

9. *Impedance Spectroscopy—Emphasizing Solid Materials and Systems*, (Edited by J. R. Macdonald). Wiley-Interscience, New York (1987).

10. J. R. Macdonald, *Electrochim. Acta* **35**, 1483 (1990).

11. D. R. Franceschetti, J. R. Macdonald and R. P. Buck, *J. electrochem. Soc.*, **138**, 1368 (1991).

12. J. R. Macdonald and L. D. Potter Jr, *Solid St. Ionics* **23**, 61 (1987).

13. J. R. Macdonald and R. L. Hurt, *J. chem. Phys.* **87**, 496 (1986).

14. L. Kirkup and J. Sutherland, *Comp Phys.* **2**, 64 (1988).

15. Y. Sakamoto, M. Ishiguro and G. Kitagama, *Akaike Information Criterion Statistics.* KTK Scientific Publishers, Tokyo, (D. Reidel, Dordrecht) (1986).